

# Carbon-nitrogen coupling on Pt(111) and its relevance to the catalytic synthesis of HCN

*Eldad Herceg and Michael Trenary\**

*Department of Chemistry, University of Illinois at Chicago, 845 West Taylor Street,  
Chicago, Illinois 60607-7061, USA*

Received: 30-11-05 Accepted: 19-02-06

## Abstract

The surface chemistry of carbon-nitrogen coupling is of fundamental importance to the industrial-scale catalytic synthesis of HCN from  $\text{CH}_4$  and  $\text{NH}_3$  over Pt gauze catalysts. In order to elucidate the details of the synthesis, we investigated the mechanism of CN bond formation on Pt(111) with reflection absorption infrared spectroscopy (RAIRS) and temperature programmed desorption (TPD). The relevant surface intermediates were generated through the thermal decomposition of  $\text{CH}_3\text{I}$  or  $\text{C}_2\text{H}_4$  and the electron induced dissociation or oxydehydrogenation of  $\text{NH}_3$ . The formation of surface CN is detected through HCN desorption at 500 K in the TPD experiments. The appearance of the vibrational features characteristic of the aminocarbyne ( $\text{CNH}_2$ ) species upon hydrogenation of surface CN at 300 K in the RAIR spectra has been used to establish the CN bond formation temperature. The RAIRS results indicate that HCN desorption at 500 K is kinetically limited by the formation of the CN bond at this temperature from surface C and N atoms. The formation of CN is suppressed in the presence of high coverages of surface carbon, in agreement with previous model reactor kinetic studies. In contrast, the coverage and overlayer structure of surface nitrogen has a negligible influence on the coupling reaction. Our results indicate that the high temperatures used in the industrial synthesis of HCN are needed primarily to activate methane and ammonia dissociative adsorption on the Pt catalyst surface.

**Key words:** Pt(111), infrared absorption spectroscopy, temperature programmed desorption, aminocarbyne, hydrogen cyanide synthesis.

## Acoplamiento carbon-nitrógeno sobre Pt(111) y su importancia en la síntesis catalítica de HCN

### Resumen

La química superficial del acoplamiento carbono-nitrógeno es de fundamental importancia a escala industrial en la síntesis de HCN a partir de  $\text{CH}_4$  y  $\text{NH}_3$  sobre catalizadores de malla de Pt. Con la finalidad de dilucidar los detalles de la síntesis, nosotros investigamos la formación del enlace CN sobre Pt(111) con espectroscopía de reflexión absorción infrarroja (RAIRS) y desorción a temperatura programada (TPD). Los intermediarios superficiales relevantes fueron generados a través de la descomposición térmica de  $\text{CH}_3\text{I}$  o  $\text{C}_2\text{H}_4$  y la disociación inducida del electrón o oxideshidrogenación de  $\text{NH}_3$ . La formación de CN superficial es detectada a través de

\* Autor para la correspondencia. E-mail: mtrenary@uic.edu. Fax: 312-996-0431.

la desorción de HCN a 500 K en los experimentos de TPD. La aparición de las bandas vibracionales características de las especies aminocarbina ( $\text{CNH}_2$ ) sobre la hidrogenación de CN superficial a 300 K en el espectro RAIRS ha sido usada para establecer la temperatura de formación del enlace CN. Los resultados de RAIRS indican que la desorción de HCN a 500 K es limitada cinéticamente por la formación del enlace CN a esta temperatura a partir de átomos de C y N superficiales. La formación de CN es suprimida en la presencia de altas cubrimientos de carbón sobre la superficie, en concordancia con estudios previos de un modelo de reactor cinético. En contraste, el recubrimiento estructural de nitrógeno superficial tiene una influencia insignificativa sobre la reacción de acoplamiento. Nuestros resultados indican que las altas temperaturas usadas en la síntesis industrial de HCN son necesarias, primeramente para activar la adsorción disociativa de metano y amoníaco sobre la superficie del catalizador de Pt.

**Palabras clave:** Pt (111), espectroscopia de absorción infrarroja, aminocarbina, síntesis de cianida de hidrógeno.

## Introduction

Annual production of hydrogen cyanide for 2004 was over a million tons and is growing at a rate 2.7% per year. Hydrogen cyanide is used as a starting material for many products, the most important of which is nylon, which accounts for ~50% of the HCN produced each year. (1) Industrially, since the 1940s, (2) hydrogen cyanide has been synthesized from  $\text{CH}_4$ ,  $\text{NH}_3$ , and  $\text{O}_2$  in the Andrussow process, which uses Pt - 10% Rh gauze catalysts at temperatures of ~1400 K. Rhodium serves primarily as a strengthener of the gauze. In addition, the CN bond dissociates measurably at high temperatures on Rh. (3) Therefore, Rh appears to play a secondary role in the Andrussow process and here we focus on Pt only. Optimization of this important industrial process obviously leads to numerous benefits. The very first step of the optimization is to explore elementary steps involved in the formation of HCN on the catalyst surface. Ultra high vacuum (UHV) techniques employed in experiments on single crystal surfaces can provide detailed information on the elementary steps in the surface chemical reactions that underlie more complex catalytic processes. Here, we use reflection absorption infrared spectroscopy (RAIRS), temperature programmed desorption (TPD), and a Pt(111) crystal.

The kinetics of HCN formation in both the absence (4, 5) and presence (6) of  $\text{O}_2$  was studied in detail by Hasenberg and Schmidt. According to them, the addition of oxygen does not increase the total reactivity of  $\text{CH}_4$  and  $\text{NH}_3$ , but rather it increases the selectivity. They found that the main reaction that leads to HCN formation even in the presence of  $\text{O}_2$  is  $\text{CH}_4 + \text{NH}_3$ , but also that HCN can be formed from the  $\text{CH}_4 + \text{NO}$  reaction. In this paper, we will discuss the details that lie behind the first reaction. Hasenberg and Schmidt also succeeded in fitting the observed reaction rates with several Langmuir-Hinshelwood rate expressions indicating that the reaction is definitely metal catalyzed and that the key steps in the reaction occur between adsorbed species. Therefore, it should be possible to determine many of the details of the reaction mechanism through studies conducted under UHV conditions.

Both  $\text{CH}_4$  and  $\text{NH}_3$  have very small dissociative sticking probabilities on Pt(111). (7, 8, 9). Therefore, we used other means to generate the reactive surface species that form during catalytic process involving  $\text{CH}_4$  and  $\text{NH}_3$ . It has been show that this is a highly successful strategy for gaining a basic understanding of reaction mechanisms underlying heterogeneous catalysis (10). Methyl iodide ( $\text{CH}_3\text{I}$ ) provides a convenient

means to generate surface  $\text{CH}_x$  ( $x = 0, 1, 2, 3$ ) species (11, 12, 13, 14). We have found that the presence of coadsorbed iodine has minimal influence on the C-N coupling reaction (15, 16). This is in agreement with the fact that the coadsorbed iodine does not strongly influence the surface chemistry of hydrocarbons (17, 18). In a separate study of submonolayer coverages of  $\text{C}_2\text{H}_4$  on Pt(111), we have shown that C-C bond scission is feasible at temperatures above 450 K (19). Therefore, we have also used  $\text{C}_2\text{H}_4$  as a source of  $\text{CH}_x$  surface species.

Ammonia does not dissociate on Pt(111) at low pressures and temperatures. However, it has been reported that  $\text{NH}_3$  can decompose on Pt surfaces under conditions other than UHV and low temperature. For example, adsorbed  $\text{NH}_3$  on Pt(111) is readily dissociated through electron irradiation to form N, NH, and  $\text{NH}_2$  species on the surface (20) and we have also generated  $\text{NH}_y$  ( $y = 0, 1, 2$ ) species by this method (21). An alternative route for  $\text{NH}_y$  generation that was also used here is the oxydehydrogenation of  $\text{NH}_3$  (22, 23, 24). A detailed description of this process will be published elsewhere (24).

## Experimental

The experiments were performed in a stainless steel ultra high vacuum (UHV) chamber with a base pressure of  $\sim 1 \times 10^{-10}$  Torr equipped with a variety of surface science techniques. A detailed description of this system can be found elsewhere (25). It is coupled to a commercial Fourier transform infrared (FTIR) spectrometer (Bruker IFS 66 v/S). A tungsten source was used in combination with an InSb detector to achieve maximum sensitivity for the RAIR spectra presented here, which are confined to the CH and NH stretch regions. In cases where the sample was annealed to a temperature above 85 K, the sample was then cooled back to 85 K before the spectrum was acquired. The background reference spectrum was also taken at 85 K. The Pt(111) surface was cleaned and judged free of impurities by

a standard procedure described earlier (26). Ammonia (99.9992%), oxygen (99.998%), hydrogen (99.9999%), and ethylene (99.99%) were purchased from Matheson Tri-gas, Inc., and were used without further purification. Methyl iodide was purchased from Alfa Aesar Co. with a quoted purity of 99.5 % and was further purified by a procedure described in detail elsewhere (13). Exposures of  $\sim 0.2$  L, 2.5 L, and 2.0 L were necessary to saturate the first layer of  $\text{NH}_3$ ,  $\text{CH}_3\text{I}$ , and  $\text{C}_2\text{H}_4$ , respectively. These coverages are correlated with the absolute coverages by comparison with data available in the literature (9, 11, 27). The exposure of 2 L of  $\text{O}_2$  at 85 K was sufficient to saturate the molecular state of oxygen (0.44 ML) on the clean Pt(111) surface (28, 29). For the experiments involving electron-induced dissociation of ammonia, an electron exposure of  $\sim 2 \times 10^{15}$  electrons per  $\text{cm}^2$  and a beam energy of 100 eV were used.

## Results

Figures 1 b) – d) show  $m/e = 27$  (HCN) TPD traces for three different  $\text{CH}_3\text{I}$  and  $\text{NH}_3$  dosing and electron exposure sequences, all with the Pt(111) surface at 85 K. The HCN desorption at  $\sim 500$  K (peak centered at 497 K) confirms that C-N bond formation can be induced on Pt(111) under UHV conditions from  $\text{CH}_3$  and  $\text{NH}_3$  fragments. Here we assume that the  $m/e = 27$  peak is due to HCN rather than the less stable isomer HNC, although there is no direct proof of this assumption. The results in Figure 1 b) were obtained after first exposing the surface to 0.2 L of  $\text{NH}_3$ , then subjecting the  $\text{NH}_3$  layer to electron irradiation, followed by exposure to 0.2 L of  $\text{CH}_3\text{I}$ . This shows that electron irradiation is needed only to induce  $\text{NH}_3$  dissociation. This is expected since  $\text{CH}_3\text{I}$  thermally dissociates on its own on Pt(111). We find, by comparison with the thermal decomposition of  $\text{CH}_3\text{I}$ , (11, 30) that exposure to the electron beam does not exert a strong influence on the surface chemistry of this molecule. Traces c) and d) in Figure 1 show

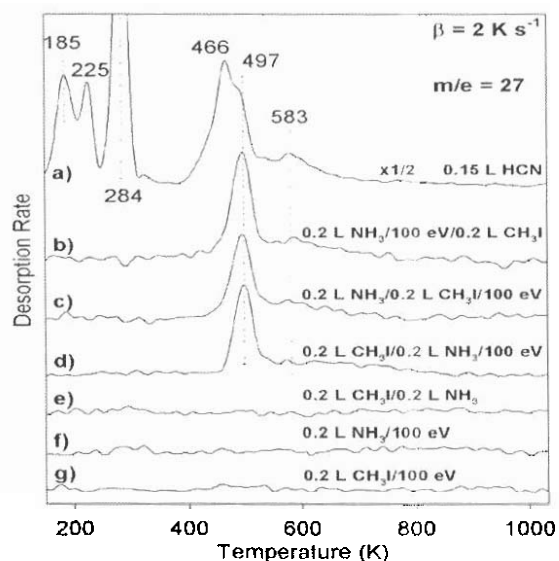


Figure 1. HCN TPD spectra for: a) 0.15 L HCN exposure at 85 K; b) – d) indicated orders of 0.2 L CH<sub>3</sub>I, 0.2 L NH<sub>3</sub>, and 100 eV exposure at 85 K; e) exposure of 0.2 L CH<sub>3</sub>I and 0.2 L NH<sub>3</sub> at 85 K; f) 0.2 L NH<sub>3</sub> electron irradiated at 85 K; and g) 0.2 L CH<sub>3</sub>I electron irradiated at 85 K.

little difference in the  $m/e=27$  signal when both NH<sub>3</sub> and CH<sub>3</sub>I are e<sup>-</sup> irradiated. Traces e) – g) are control experiments that show that the HCN desorption in Figures b) – d) is not an artifact related to e<sup>-</sup> beam exposure. The absence of HCN desorption in the absence of e<sup>-</sup> beam exposure, Figure 1 e), shows that C–N coupling does not occur from a reaction of CH<sub>3</sub> and NH<sub>3</sub>, but rather from their dissociation products. Figure 1 a) shows the  $m/e=27$  result following exposure to 0.15 L of HCN at 85 K, which agrees with previous results (31, 32). The highest temperature peaks in Figure 1 a) are at 466 K, with a shoulder at 497 K, and at 583 K, with the latter peak part of a high-temperature tail. For the HCN desorption traces in Figures 1 b) – d), there is also a high temperature tail. This indicates that this high temperature tail is not specific to the C–N coupling reaction. In a TPD study of HCN on the Pt(111) and stepped Pt(211) sur-

faces, (32) the high temperature tail was observed to be much more intense for the latter, indicating that it is associated with step sites.

TPD traces of the other relevant desorption products in the course of CN bond formation on Pt(111) have also been monitored and they provide further insight into the C–N coupling reaction. Specifically, we observed decreases in the desorption of N<sub>2</sub> and H<sub>2</sub> above 450 K when compared to the desorption of N<sub>2</sub> and H<sub>2</sub> following electron irradiation of only NH<sub>3</sub> or of only CH<sub>3</sub>I. This has been attributed to the consumption of surface N atoms by the CN bond formation reaction and the loss of hydrogen through HCN desorption (15).

The use of RAIRS to detect the presence of surface CN and the C–N bond formation temperature is demonstrated in Figure 2. After exposing the Pt(111) surface to 0.2 L of CH<sub>3</sub>I and 0.2 L NH<sub>3</sub> at 85 K, it was irradiated with 100 eV electrons and annealed to 450, 500, and 550 K. After each anneal, the sample was cooled to 300 K, exposed to 10 L of H<sub>2</sub>, then cooled to 85 K where the spectra were acquired. As previous work has shown, (26) if there is CN on the Pt(111) surface, then an H<sub>2</sub> exposure at 300 K should produce CNH<sub>2</sub>, with an NH symmetric stretch in the range of 3365–3370 cm<sup>-1</sup>. The 450 K anneal yields an intense peak at 3312 cm<sup>-1</sup>, which grows in intensity and shifts to 3315 cm<sup>-1</sup> after the H<sub>2</sub> exposure. This peak is due to the NH species and its formation and properties have been described in detail elsewhere (21). There is no peak due to CNH<sub>2</sub> for the 450 K anneal nor for any annealing temperatures below 450 K. The 500 K anneal induces dissociation of the NH species which eliminates the  $\mu(\text{NH})$  peak. This peak reappears at 3311 cm<sup>-1</sup> after H<sub>2</sub> exposure due to rehydrogenation of surface N atoms. In addition,  $\mu(\text{NH})$  of the CNH<sub>2</sub> species now appears at 3370 cm<sup>-1</sup>, demonstrating that the 500 K anneal leads to the formation of CN on the surface. We do not observe an asymmetric NH stretch of CNH<sub>2</sub> and this is

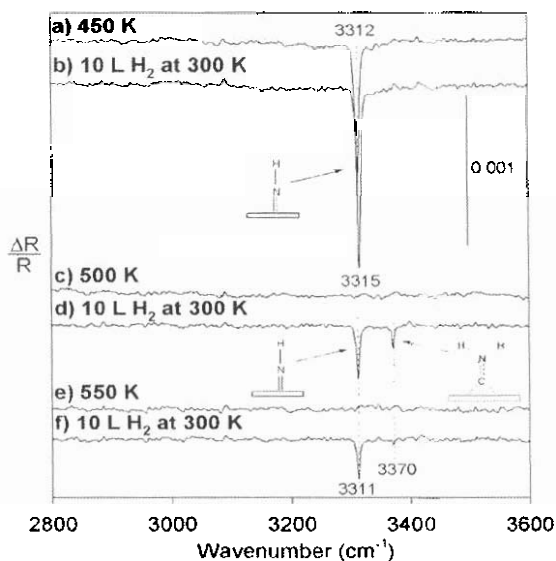


Figure 2. RAIR spectra obtained after exposing 0.2 L of CH<sub>3</sub>I and 0.2 L of NH<sub>3</sub> to the sample at 85 K followed by e<sup>-</sup> beam irradiation with subsequent heating to the indicated temperatures and exposure to 10 L of H<sub>2</sub> at 300 K.

in agreement with the fact that for CNH<sub>2</sub> bonded to the surface at a twofold bridge site with the CN axis along the surface normal, (33) only one peak in the N-H stretch region should be observed according to the surface selection rule. The  $\mu(\text{NH})$  peak of CNH<sub>2</sub> is still present after a 550 K anneal, but has a lower intensity presumably due to removal of CN by HCN desorption through reaction of CN with background hydrogen.

Hasenberg and Schmidt (5) have shown that the HCN yield strongly depends on the surface carbon coverage. Therefore, we investigated the dependence of HCN yield from a series of TPD experiments where we varied the CH<sub>x</sub> coverage for a fixed initial NH<sub>3</sub> coverage. The results are shown in Figures 3 a) and b). The HCN yield is defined as the area of the m/e = 27 TPD peak. A monolayer (ML) is defined here as the saturated first layer of NH<sub>3</sub> ( $\alpha\text{-NH}_3$ ), CH<sub>3</sub>I, or C<sub>2</sub>H<sub>4</sub>. By this definition, 1 ML of ammonia, methyl iodide, and

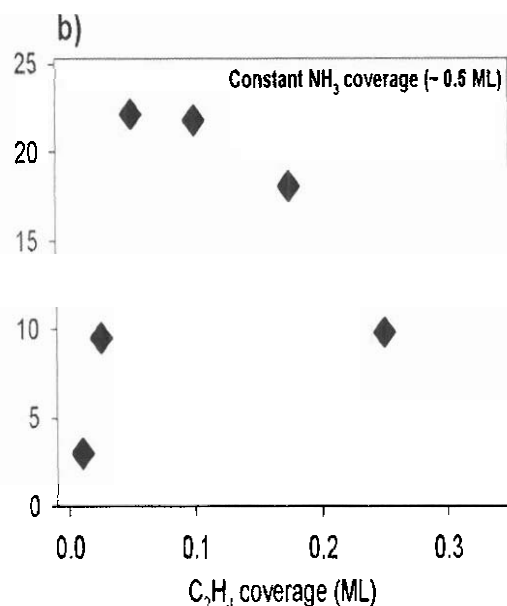
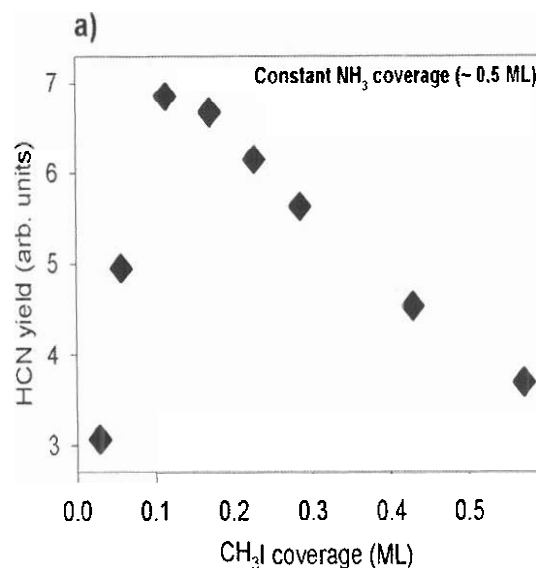


Figure 3. a) HCN yield as a function of CH<sub>3</sub>I coverage for a fixed initial NH<sub>3</sub> coverage of ~0.5 ML; b) HCN yield as a function of C<sub>2</sub>H<sub>4</sub> coverage for a fixed initial NH<sub>3</sub> coverage of ~0.5 ML.

ethylene corresponds to one molecule per 4, 5 and 4 surface Pt atoms, respectively (9, 11, 27). The initial NH<sub>3</sub> coverage of approxi-

mately 0.5 ML was achieved by a 0.1 L exposure of  $\text{NH}_3$  at 85 K. For Figure 3 a), the surface was then bombarded with 100 eV electrons and exposed to different amounts of  $\text{CH}_3\text{I}$ . The HCN yield reaches a maximum for 0.10 – 0.15 ML of  $\text{CH}_3\text{I}$  after which it drops significantly, implying that either  $\text{CH}_3\text{I}$  itself, or one of its dissociation products, causes the quenching of the C–N coupling reaction. Figure 3 b) shows the HCN yield as a function of initial  $\text{C}_2\text{H}_4$  coverage for an initial ammonia coverage of 0.5 ML. A similar dependence of HCN yield on  $\text{C}_2\text{H}_4$  coverage is observed as in Figure 3 a), indicating that a low carbon coverage is most favorable for HCN production. The comparison between  $\text{C}_2\text{H}_4$  and  $\text{CH}_3\text{I}$  in Figure 3 shows that coadsorbed iodine does not exert a strong influence on CN bond formation. The benign role of iodine was also established in experiments in which HCN was observed through the reaction of N atoms with surface carbon deposited through  $\text{CH}_3\text{I}$  dissociation and annealing to a temperature high enough to desorb iodine (15).

The poisoning at high carbon coverages also has been investigated with RAIRS as shown in Figure 4. Before spectra a) – c) were acquired at 85 K, the surface was first exposed to 0.2 L of  $\text{NH}_3$ , electron irradiated, and exposed to the indicated amounts of  $\text{CH}_3\text{I}$  at 85 K. The crystal was then annealed to 500 K to induce the C–N coupling reaction, cooled back to 300 K and exposed to 10 L of  $\text{H}_2$  in order to form the  $\text{CNH}_2$  species. Two peaks appear in each spectrum in Figure 4 and their assignment is the same as for the peaks in Figure 2 d). The peak corresponding to aminocarbene ( $3370\text{ cm}^{-1}$ ) has the highest intensity for the lowest initial  $\text{CH}_3\text{I}$  coverage and it gradually decreases with the increase in  $\text{CH}_3\text{I}$  coverage. The peak intensity for 0.6 L  $\text{CH}_3\text{I}$  is about half of what is observed for 0.2 L  $\text{CH}_3\text{I}$ , in good agreement with the TPD results shown in Figure 3 a). Spectrum d) in Figure 4 was obtained in a similar manner, except that 0.4 L of a 1:1 gas phase mixture of  $\text{NH}_3$  and  $\text{CH}_3\text{I}$  was exposed to Pt(111) at 85 K and then the surface was electron irradiated.

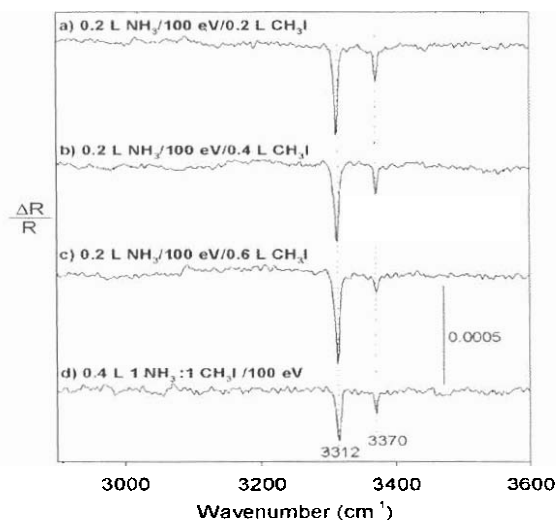


Figure 4. a) – c) RAIR spectra of Pt(111) after annealing 0.2 L of  $\text{NH}_3$  exposed to 100 eV electrons and indicated amounts of  $\text{CH}_3\text{I}$  to 500 K, cooling back to 300 K and exposing to 10 L of  $\text{H}_2$ ; d) RAIR spectrum after annealing the surface exposed at 85 K to 0.4 L of a 1:1 gas phase mixture of  $\text{NH}_3$  and  $\text{CH}_3\text{I}$  to 500 K, cooling and exposing to 10 L of  $\text{H}_2$  at 300 K.

The purpose of this experiment was to control for the possibility that the  $\text{CH}_3\text{I}$  and  $\text{NH}_3$  might segregate into separate islands. If not thoroughly mixed, then the C–N coupling reaction might occur only at boundaries between C- and N-containing islands. For example, it is well known that surface carbon becomes mobile at higher temperatures and forms unreactive graphitic islands (11, 34). The  $3370\text{ cm}^{-1}$  peak in d) is about the same as in b), showing that simultaneous exposure to  $\text{CH}_3\text{I}$  and  $\text{NH}_3$  yields the same result as sequential exposure, making the possibility that the reaction occurs only at islands edges less likely. Even if there is aggregation of surface species into separate islands on the surface, it must be a characteristic of the surface chemistry of the parent molecules rather than a consequence of sequential dosing.

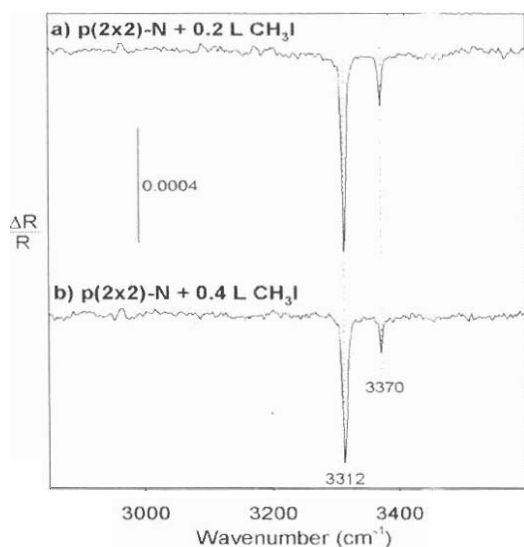


Figure 5. Before acquiring IR spectra in a) and b) Pt(111) was covered with a p(2x2) nitrogen overlayer, exposed to indicated amounts of CH<sub>3</sub>I, annealed to 500 K, cooled back to 300 K and exposed to 10 L of H<sub>2</sub>. The p(2x2)-N covered surface was prepared by dosing of 2.0 L O<sub>2</sub> and 0.4 L NH<sub>3</sub> at 85 K and annealing Pt(111) to 400 K for 60 seconds.

The influence of surface nitrogen on the CN bond formation has been investigated by RAIRS and the results are presented in Figure 5. Before taking a spectrum at 85 K, the surface was first covered with a p(2 × 2)-N layer, exposed to the indicated amounts of CH<sub>3</sub>I, annealed to 500 K, cooled back to 300 K, where it was exposed to 10 L of H<sub>2</sub>. The p(2 × 2)-N layer has been prepared by the following method: the Pt(111) surface was held at 85 K, exposed to 2.0 L of O<sub>2</sub> and 0.4 L of NH<sub>3</sub>, and then annealed to 400 K for 60 seconds. This yields a surface covered only with N atoms as determined by Auger electron spectroscopy and a sharp p(2 × 2) LEED pattern. We have found that ~ 25% more nitrogen is present on the surface by

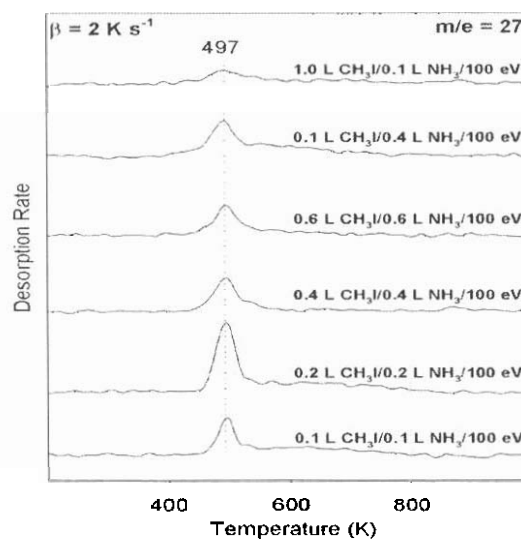


Figure 6. HCN TPD spectra after electron irradiation of Pt(111) exposed to indicated amounts of CH<sub>3</sub>I and NH<sub>3</sub> at 85 K.

this route when compared to the electron-induced dissociation of NH<sub>3</sub>. A detailed description of the formation and surface properties of a p(2 × 2)-N layer on Pt(111) can be found elsewhere (24). As before, two peaks appear in the N-H stretch region. In Figure 5 a), the intensity of the peak at 3370 cm<sup>-1</sup> due to CNH<sub>2</sub> is the same as for the peak in Figure 4 a), indicating that the different surface structure and coverage of the nitrogen atoms do not influence the CN bond formation, in contrast to what was observed for surface carbon atoms.

Figure 6 shows HCN desorption for different NH<sub>3</sub> and CH<sub>3</sub>I exposures. It can be seen that the peak temperature does not change for different amounts of HCN evolving from the surface. This is an indication of first-order desorption kinetics. Therefore, a more complex sequence of events leads to HCN desorption than simply through the CN + H reaction since this would imply second-order kinetics.

## Discussion

Based on thermodynamics, the endothermic reaction of HCN formation from  $\text{CH}_4$  and  $\text{NH}_3$  should not occur at all at temperatures below  $\sim 1000$  K since this reaction has an equilibrium constant,  $K_{\text{eq}} \ll 1$  for  $T < 1000$  K. (3) For instance, at 600 K  $K_{\text{eq}}$  is  $\sim 10^{-10}$ . However, in our experiments we bypass the most endothermic steps in the reaction, namely the breaking of the first C-H and N-H bonds of  $\text{CH}_4$  and  $\text{NH}_3$ , respectively. This permits the C-N coupling reaction and hence the HCN formation reaction to occur at much lower temperatures in our experiments than in catalytic reactors. Desorption of HCN at  $\sim 500$  K in Figures 1 b) - d) is consistent with CN bond formation at or below this temperature. The appearance of the  $\text{CNH}_2$  peak at  $3370 \text{ cm}^{-1}$  in the RAIRS spectrum shown in Figure 2 d), after hydrogenation of the surface at 300 K following the 500 K anneal, shows that the CN bond is formed at  $\sim 500$  K.

Dehydrogenation of  $\text{CH}_3$  on Pt(111) to surface carbon atoms is complete by  $\sim 460$  K (11-15). This is confirmed by the absence of any C-H stretching frequencies in Figure 2 c). Therefore, we identify surface C atoms from methyl as the reactive carbon-containing species involved in the C-N coupling reaction. Our previous studies have shown that NH molecules are completely dissociated at 500 K to surface N atoms (15, 21). (15, 21) Disappearance of the NH stretch peak at  $3315 \text{ cm}^{-1}$ , Figure 2 c), confirms this. Surface N atoms are therefore the nitrogen-containing species involved in the coupling reaction. Desorption of HCN in our TPD experiment indicates that surface CN formed from C and N atoms is hydrogenated to some extent at 500 K. Since this is above the recombinative desorption of  $\text{H}_2$ , the hydrogen must originate from the decomposition of surface CH and/or NH species. As already noted, dehydrogenation of the NH species is complete well before 500 K (15, 21). On the other hand, we observed a high-temperature tail up to 550 K in the  $\text{H}_2$  desorption for the peak corresponding to the decomposition of

CH (15). This indicates that the source of hydrogen in the HCN desorption originates from the dissociation of CH.

Kinetic studies have shown that HCN synthesis is feasible when the surface contains less than a monolayer of carbon and that it even can be stopped completely in the case of a carbon multilayer (5). Therefore, we investigated the influence of  $\text{CH}_x$  coverage on the C-N bond formation, Figures 3 and 4. For a given initial coverage of nitrogen, the stoichiometry of the reaction  $\text{CH}_3 + \text{NH}_3 \rightarrow \text{HCN} + 5/2 \text{H}_2$  implies that the maximum HCN yield should occur when the carbon coverage equals the nitrogen coverage. This assumes that there is uniform mixing of the reactants, which as described earlier is supported by the spectrum presented in Fig. 4d). For our initial coverage of 1  $\text{NH}_3$  per 8 surface atoms, we expect that the amount of HCN formed should increase steadily up to coverage of 1  $\text{CH}_3$  per 8 Pt atoms. However, in Figure 3 a) the HCN yield decreases significantly for a much lower coverage of  $\text{CH}_3$ , i.e. 1  $\text{CH}_3$  per every 50 surface atoms, which is by a factor of  $\sim 6$  below what is implied by the stoichiometry. Figure 3 b) shows that a molecule that does not contain iodine,  $\text{C}_2\text{H}_4$ , showed a similar dependence of HCN yield on carbon coverage. This strongly suggests that surface carbon is responsible for deactivation of the surface, in agreement with the kinetic studies performed by Hasenberg and Schmidt (5). The amount and structure of surface nitrogen on Pt(111), on the other hand, did not influence the CN yield as seen by comparison of the peak intensities at  $3370 \text{ cm}^{-1}$  in Figures 4 a) and 5 a).

In the case of the C-N coupling reaction, the HCN desorption temperature, as observed with TPD, and the  $\text{CNH}_2$  formation and dissociation temperature, as observed with RAIRS, can be compared with similar observations when the CN bond is already present, such as when HCN or methyl amine is dosed onto the surface at low temperature. In the latter cases the CN bond remains intact and CN is eventually removed from the

surface through the desorption of either HCN or cyanogen,  $C_2N_2$ . From the results presented here and in previous studies by our group (26-, 31), it is known that  $CNH_2$  dissociates between 400 and 500 K on Pt(111) and leads to desorption of HCN in the range of 450–600 K. The  $CNH_2$  species has also been identified on other surfaces including Rh(111) following the thermal decomposition of methyl amine (35) and on oxides and on oxide supported Rh catalysts from the hydrogenation of HCN (36). The close correspondence between the temperature at which  $CNH_2$  decomposes and the temperature at which HCN desorbs, suggests that when the surface is covered with  $CNH_2$ , its dissociation is the rate limiting step for HCN desorption. Since HCN or HNC is not observed with RAIRS when  $CNH_2$  dissociates, it follows that breaking of the first N-H bond is the rate-limiting step, followed by the rapid isomerization of the resulting HNC to HCN, which then immediately desorbs. The relatively high temperature observed following the coupling reaction for the desorption of HCN, suggests that the kinetics of the latter process is limited by the CN formation rate. Whether the HCN desorption then proceeds by way of  $CNH_2$  or by way of a transient HNC or HCN species is difficult to determine with the type of RAIRS experiments performed here, which only detect stable, rather than transient, intermediates.

### Summary

We explored elementary steps involved in the formation of HCN on Pt(111) from  $CH_x$  and  $NH_y$ . The experimental results show that individual C and N atoms are the surface species involved in the carbon-nitrogen-coupling reaction. The coupling between C and N atoms on the Pt(111) surface occurs at  $\sim 500$  K. Formation of surface CN is strongly dependent on carbon coverage, in agreement with previous kinetic studies.

### Acknowledgment

We gratefully acknowledge support by a grant from the National Science Foundation (CHE-0135561).

### References

1. SATTERFIELD, C.N. *Heterogeneous Catalysis in Practice*, Mc Graw Hill; New York, 1980.
2. SCHMIDT L.D., HICKMAN, D.A. in *Catalysis of Organic Reactions*; Kosak, J. R.; Johnson, T. A., Eds.; Marcel Dekker, Inc.: New York, 1994, 195.
3. HASENBERG D., SCHMIDT L.D. *J Catal* 1985, 91, 116.
4. HASENBERG D., SCHMIDT L.D. *J Catal* 1986, 97, 156.
5. HASENBERG D., SCHMIDT L.D. *J Catal* 1987, 104, 441.
6. UKRAINTSEV V.A., HARRISON I. *Surf Sci* 1993, 286, L571. MELXNER D.L., GEORGE S.M. *Surf Sci* 1993, 297, 27. ALBERAS-SLOAN D.J., WHITE J.M. *Surf Sci* 1996, 365, 212.
7. SEXTON B.A., MITCHELL G.E. *Surf Sci* 1980, 99, 523.
8. FISHER G.B. *Chem Phys Lett* 1981, 79, 452.
9. BENT B.E. *Chem Rev* 1996, 96, 1361.
10. ZAERA F., HOFFMANN H. *J Phys Chem* 1991, 95, 6297.
11. HENDERSON M.A., MITCHELL G.E., WHITE J.M. *Surf Sci Lett* 1987, 184, L325.
12. HERCEG E., CELIO H., TRENARY M. *Rev Sci Instrum* 2004, 75(8), 2545.
13. SOLYMOSI F., RÉVÉSZ K. *J Am Chem Soc* 1991, 113, 9145.
14. HERCEG E., TRENARY M. *J Phys Chem B* 2005, 109, 17560.
15. HERCEG E., TRENARY M. *J Am Chem Soc* 2003, 125, 15758.

16. FAIRBROTHER D.H., PENG X.D., VISWANATHAN R., STAIR P.C., FAN J., TRENARY M. *Surf Sci* 1993, 285, L455.
17. FAN J., TRENARY M. *Langmuir* 1994, 10, 3649.
18. DENG R., HERCEG E., TRENARY M. *Surf Sci* 2004, 573(2), 310.
19. BURNS A.R., STECHEL E.B., JENNISON D.R., LIY.S. *J Chem Phys* 1994, 101, 6318. Sun Y.M., SLOAN D., IHM H., WHITE J.M. *J Vac Sci Technol A* 1996, 14, 1516. BATER C., CAMPBELL J.H., CRAIG JR. J.H. *Surf Interface Anal* 1998, 26, 97.
20. HERCEG E., MUDIYANSELAGE K., TRENARY M. *J Phys Chem B* 2005, 109, 2828.
21. AMORELLI T.S., CARLEY A.F., RAJUMON M.K., ROBERTS M.W., WELLS, P.B. *Surf Sci* 1994, 315, L990.
22. MIEHER W.D., HO, W. *Surf Sci* 1995, 322, 151.
23. HERCEG E., JONES J., MUDIYANSELAGE K., TRENARY M. (to be published).
24. BRUBAKER M.E., TRENARY M. *J Chem Phys* 1986, 85, 6100.
25. JENTZ D., CELIO H., MILLS P., TRENARY M. *Surf Sci* 1995, 341, 1.
26. MITCHELL I.V., LENNARD W.N., GRIFFITHS K., MASSOUMI G.R., HUPPERTZ J.W. *Surf Sci* 1991, 256(1-2), L598.
27. STEININGER H., LEHWALD S., IBACH H. *Surf Sci* 1982, 123, 1.
28. AVERY N.R. *Chem Phys Lett* 1983, 96, 371.
29. HENDERSON M.A., MITCHELL G.E., WHITE J.M. *Surf Sci* 1991, 248, 279.
30. CELIO H., MILLS P., JENTZ D., PAE Y.I., TRENARY M. *Langmuir* 1998, 14, 1379.
31. HAGANS P.L., GUO X., CHORKENDORFF I., WINKLER A.; SIDDIQUI H., YATES JR. J.T. *Surf Sci* 1988, 203, 1
32. CHATTERJEE B.; KANG D. -H.; HERCEG E.; TRENARY M. *J Chem Phys* 2003, 199, 10930.
33. LAND T.A., MICHELY T., BEHM R.J.; HEMMINGER J.C., COMSA G. *J Chem Phys* 1992, 97(9), 6774. SMIRNOV M. YU., GORODETSKII V.V., CHOLACH A.R., ZEMLYANOV D. YU. *Surf Sci* 1994, 311, 308.
34. BOL C.W.J., KOVACS J.D., CHEN M., FRIEND C.M. *J Phys Chem B* 1997, 101, 6436.
35. RASKÓ J., BÁNSÁGI T., SOLYMOSSI, F. *Phys Chem Chem Phys* 2002, 4, 3509.